

山东大学
SHANDONG UNIVERSITY

arXiv:2610.32084

Geoneutrino Flux Prediction and Reactor Background at the JNE

Kaikai Meng

Nov 2026

Outline

1 Introduction
2 Flux Formula
3 Geophysical Model
  3.1 Mantle & Crustal Models
  3.2 SWChinaCVM-2.0
  3.3 CRUST1.0-SWChina-merged
4 Geochemical Model
5 Geoneutrino Flux at JNE
6 Reactor Background & Total IBD Spectrum
7 Summary & Outlook

1. Introduction

Earth surface heat flow: 46 ± 3 TW

Driven by radiogenic heat from HPEs (U, Th, K) + primordial energy.

Three competing BSE models:

Model	Basis	Radiogenic Heat
Low-Q	Cosmochemical (E-chondrites)	11 ± 2 TW
Medium-Q	Geochemical (mantle xenoliths)	20 ± 4 TW
High-Q	Geodynamical (surface heat flow)	33 ± 3 TW

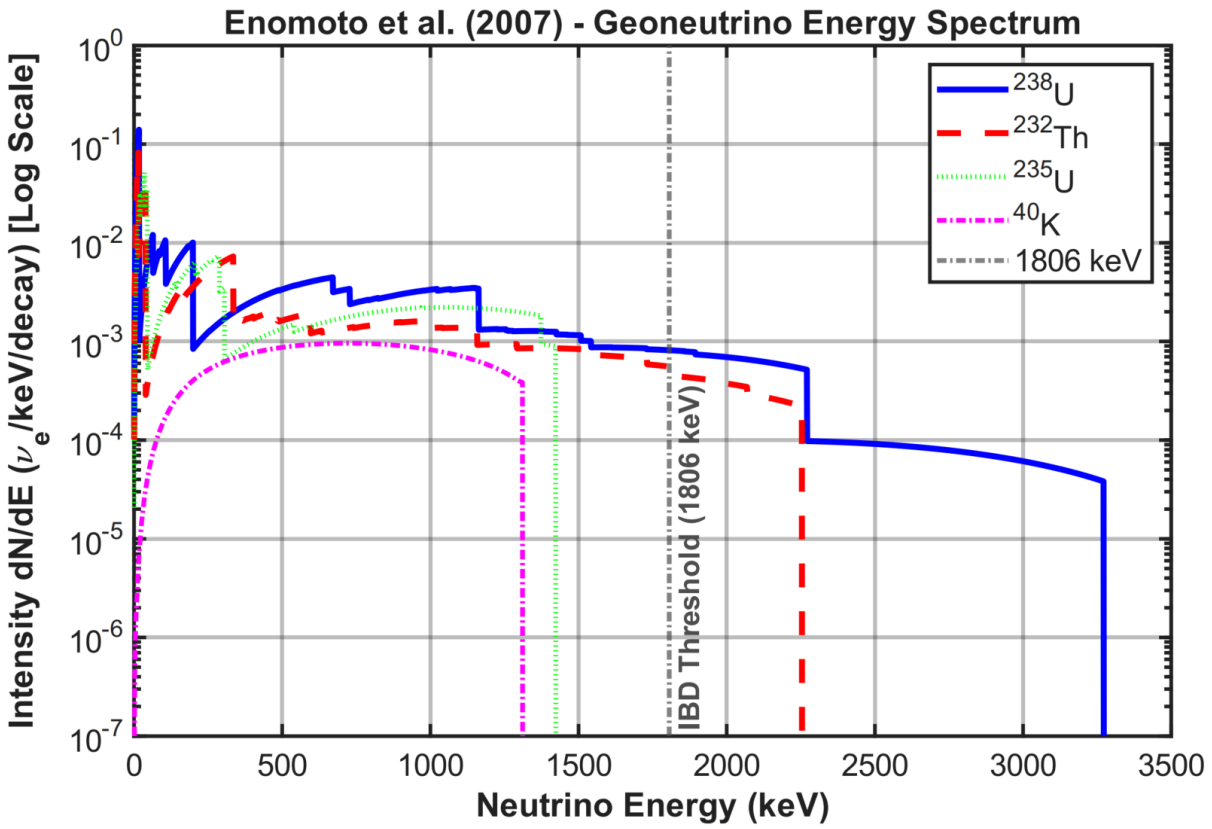

$$^{238}\mathrm{U} \rightarrow ^{206}\mathrm{Pb} + 8\alpha + 6e^{-} + 6\bar{\nu}_e + 51.7\ \mathrm{MeV},$$
$$^{235}\mathrm{U} \rightarrow ^{207}\mathrm{Pb} + 7\alpha + 4e^{-} + 4\bar{\nu}_e + 46.4\ \mathrm{MeV},$$
$$^{232}\mathrm{Th} \rightarrow ^{208}\mathrm{Pb} + 6\alpha + 4e^{-} + 4\bar{\nu}_e + 42.7\ \mathrm{MeV},$$
$$^{40}\mathrm{K} \rightarrow ^{40}\mathrm{Ca} + e^{-} + \bar{\nu}_e + 1.31\ \mathrm{MeV} \quad (89.3\%),$$
$$^{40}\mathrm{K} + e^{-} \rightarrow ^{40}\mathrm{Ar} + \nu_e + 1.51\ \mathrm{MeV} \quad (10.7\%).$$

2. Flux Formula

Differential Rate per Target Proton

$$R(E) = \phi(E)\,\sigma_{\mathrm{IBD}}(E)$$

Integrate R(E) above E_thr, then multiply by 10^{32} protons $\times$ 1 yr → signal in TNU

Differential Flux from HPE

$$\phi_i(E) = \frac{\lambda_i N_A}{\mu_i}\, n_\nu(i) \int \frac{A_i(\boldsymbol{r})\,\rho(\boldsymbol{r})}{4\pi L^2}\, P_{ee}(E,L)\, f_i(E)\, d\boldsymbol{r}$$

λ_i : decay constant N_a : Avogadro constant

μ_i : standard molar mass $n_\nu(i)$: $\bar{\nu}_e$ per decay chain

$f_i(E)$: normalized $\bar{\nu}_e$ spectrum per decay chain

Three-flavor Vacuum Oscillation

$$P_{ee}(E,L) = 1 - \cos^4\theta_{13}\,\sin^2 2\theta_{12}\,\sin^2\left(\frac{\Delta m^2_{21} L}{4E}\right) - \sin^2 2\theta_{13}\,\sin^2\left(\frac{\Delta m^2_{31} L}{4E}\right)$$

$\sin^2\theta_{12} = 0.3092 \pm 0.0087$ (JUNO 2025), others from PDG

Matter effect only ~0.3% of the signal → neglected

3 Geophysical Model

3.1 Mantle Model

Scenario	Description
① Uniform	Homogeneous composition throughout the mantle
② Layered Uniform	**Depleted upper mantle + enriched lower mantle ✓**
③ Single Enriched Blob	LLSVPs treated as one enriched layer
④ Symmetric Blobs	Two enriched blobs beneath Pacific & Africa

→ Mantle contribution robust:

only ~10% variation across all models (Šrámek et al., 2013)

Crustal Model

Model	Year	Resolution	Status
CRUST5.0	~2000	5°×5°	Too coarse
CRUST2.0	~2004	2°×2°	Too coarse
CRUST1.0 ✓	2012	1°×1°	Global standard
LITHO1.0	2014	1°×1°	Includes lithosphere
ECM1 ✓	2023	1°×1°	Updated synthesis

3.2 SWChinaCVM-2.0

Feature	Detail
Release	2022, China Seismic Experimental Site (CSES)
Coverage	Sichuan-Yunnan region (encompasses JNE site)
Resolution	0.2° × 0.2° (crust & uppermost mantle) — vs 1°×1° CRUST1.0
Data Volume	~7.06M body-wave + ~0.1M surface-wave data
Method	AI phase picking + ambient noise cross-correlation

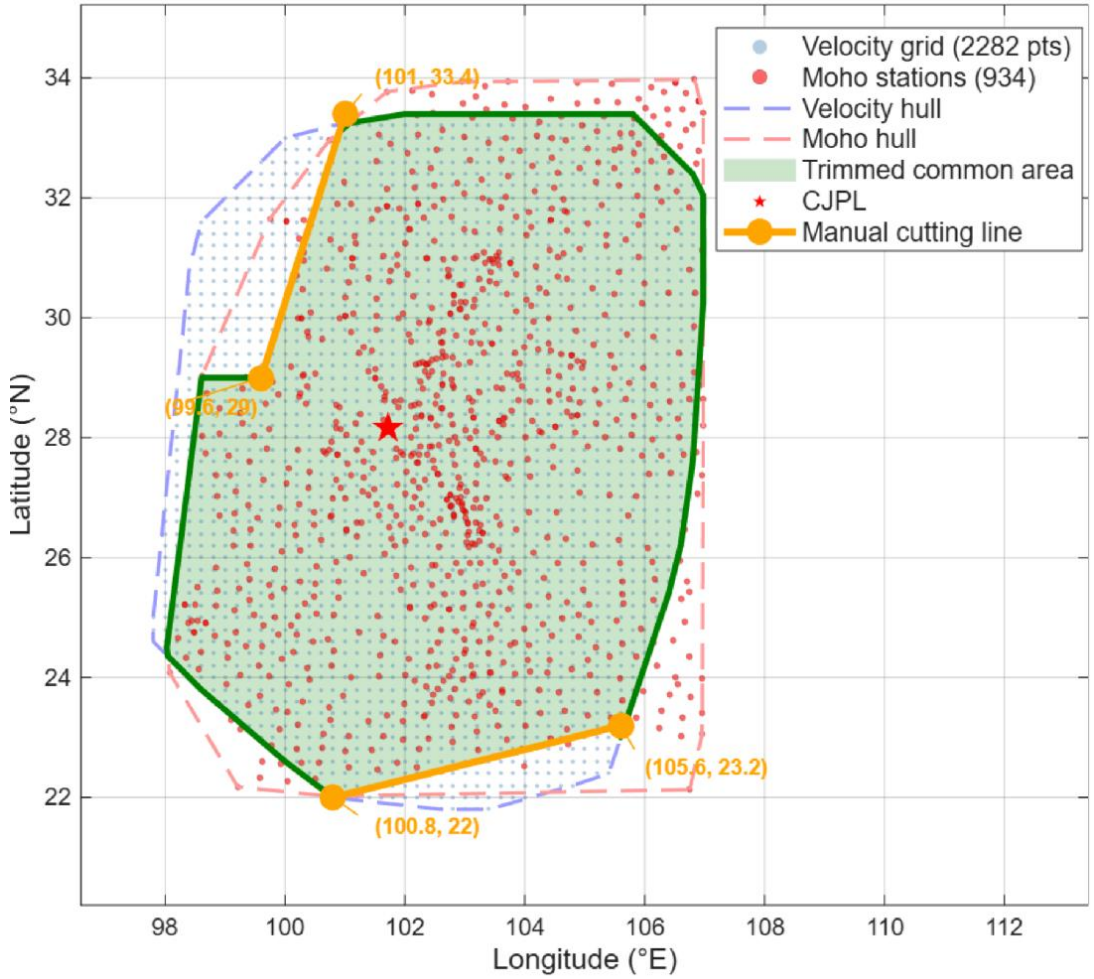

SWChinaCVM-MOHO-2.0

Integrated **3 new-generation velocity models** (SWChinaCVM-2.0, CSES-VM1.0, USTClitho2.0) → Moho interface model (incl. receiver functions)

3.3 CRUST1.0-SWChina-merged

Step 1: Moho Depth for Each 0.2° Cell

Data Source	Role
SWChinaCVM-2.0	Vp/Vs profiles at each (lon,lat,depth)
SWChinaCVM-MOHO-2.0	Crustal thickness

Step 2: Surface Elevation (ETOPO1)

CVM-2.0 issue	Reports uniform max 5 km at each grid (no real topography)
Topography source	The ETOPO1 Ice Surface data are sourced from NOAA.

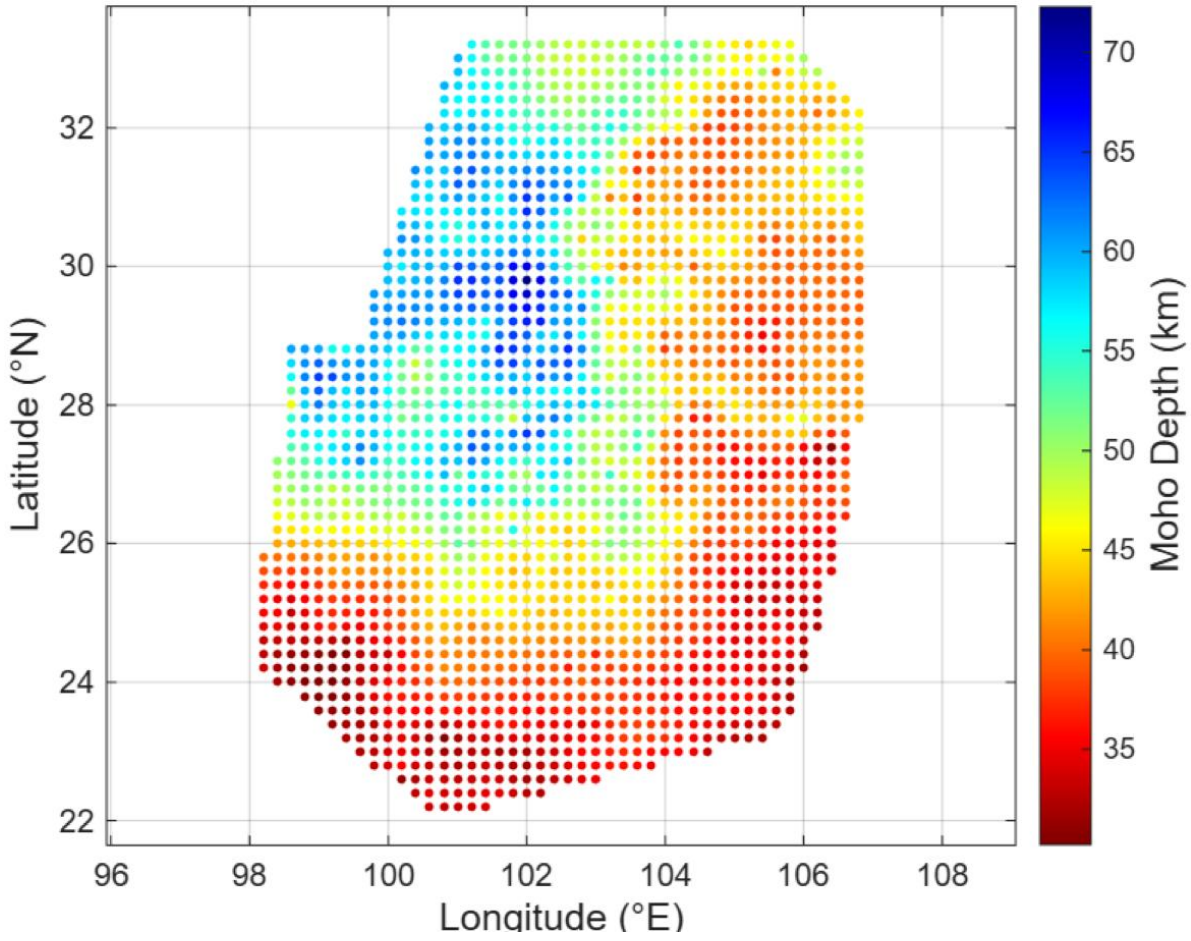

Step 3: Sediment & Crustal Proportions

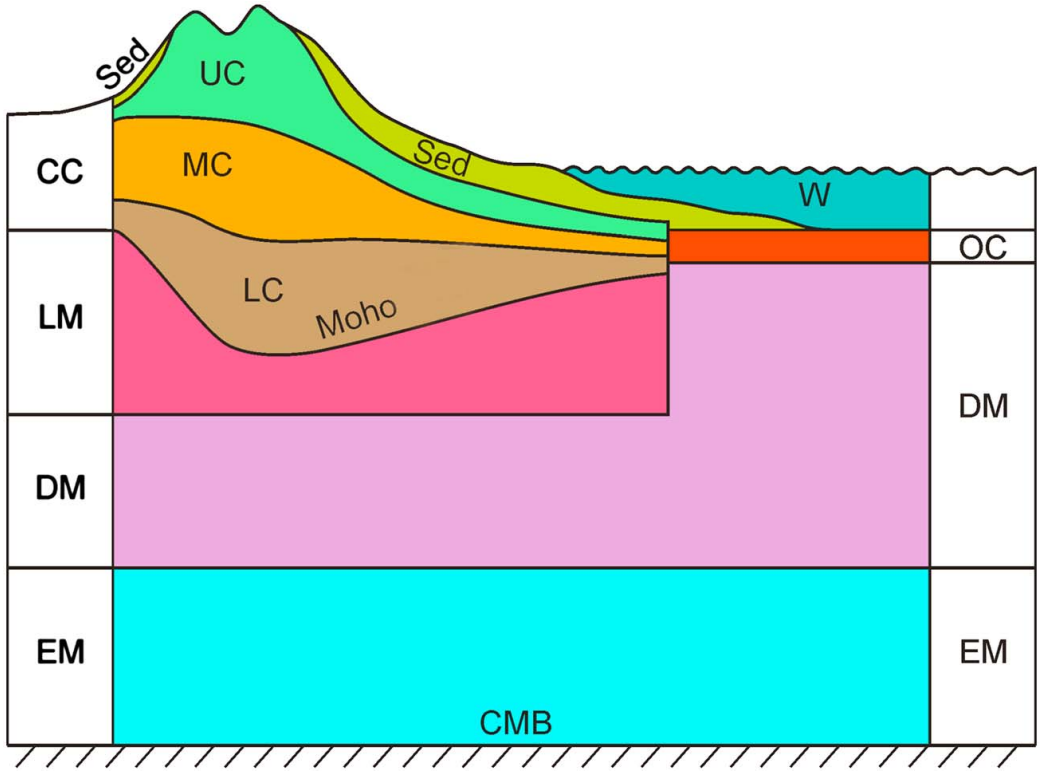

The sediment thicknesses and the relative thickness proportions of the upper, middle, and lower crystalline crust (UC, MC, and LC) are inherited from CRUST1.0.

Step 4: Merging SWChinaCVM-2.0 with CRUST1.0

CRUST1.0:
180*360 = 64,800 grid cells.

Combined model:
64,800 - 93 + 93*25 = 67,032 grid cells.

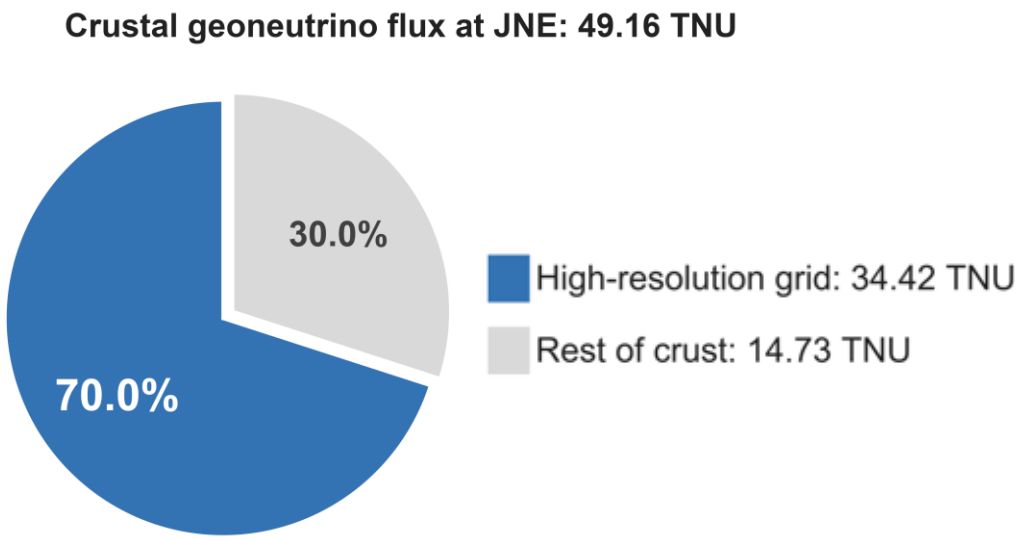

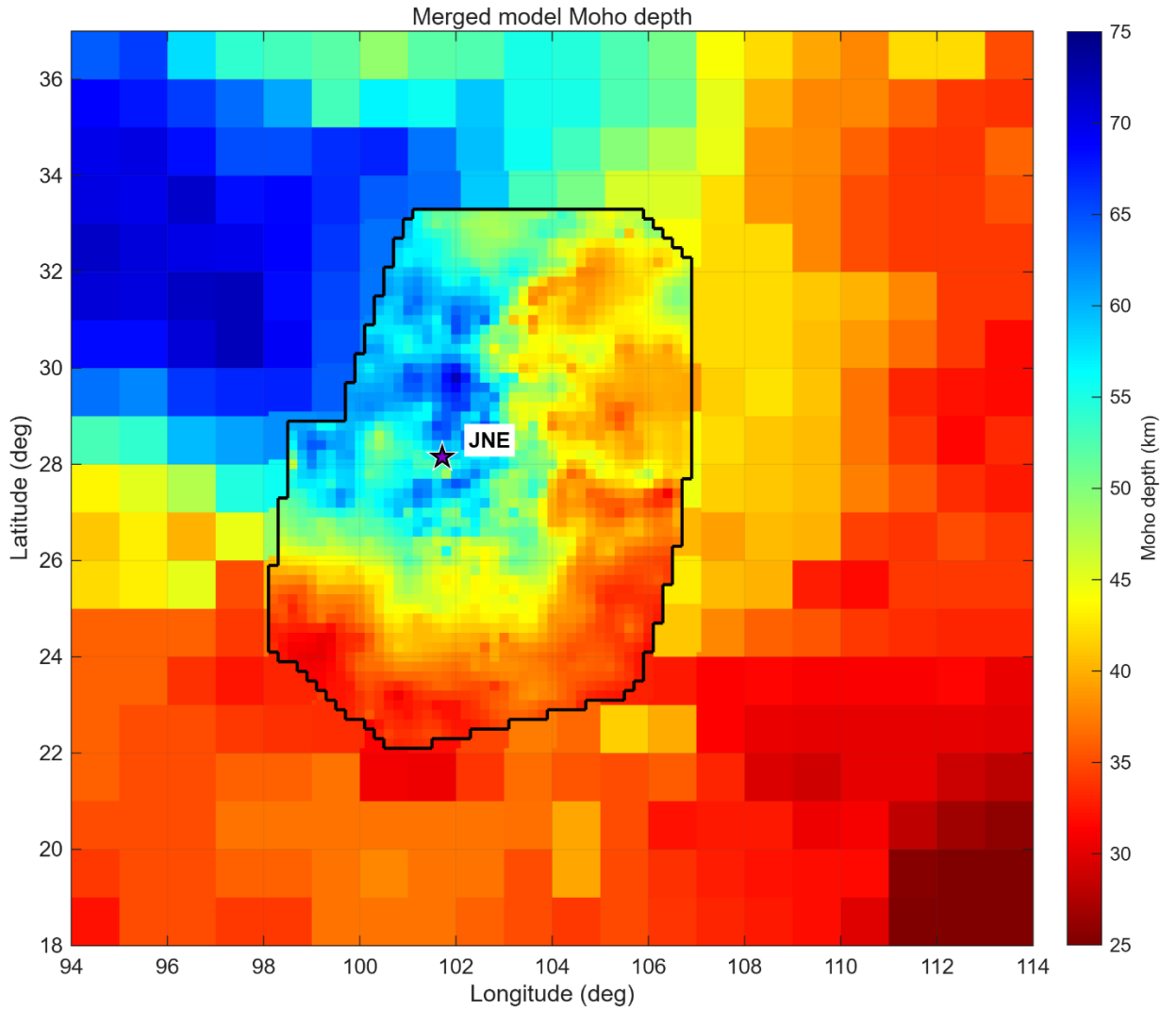

4. Geochemical Model

HPE Abundance per Layer

Layer	Source / Method
Upper Crust	Rudnick & Gao (2014) meta-analysis
Middle Crust & Lower Crust	Vp–composition fit: Equations 6, 7, and 8.
Sediments	GLOSSII model (Plank, 2014)
Oceanic Crust	Global average (White & Klein, 2014)
Lithospheric Mantle	Xenolith data (Huang et al., 2013)
Depleted Mantle (DM)	U from Arevalo et al. (2013); Th, K from MORB Th/U and K/U ratios
Enriched Mantle (EM)	**mass balance from BSE minus lithosphere and DM**

Vp–Composition Linear Relationship

Binary felsic-mafic mixture: Vp and HPE abundances as weighted averages

$$V_{\text{model}} = V_f f + V_m m \tag{6}$$

$$1 = f + m \tag{7}$$

$$a_{\text{output}} = a_f f + a_m m \tag{8}$$

where V_f, V_m, a_f, and a_m are the V_P and abundance of the felsic and mafic endmembers of amphibolite (middle crust) and granulite (lower crust), V_{model} is the V_P provided by the geophysical model, and f and m are the mass proportions of felsic and mafic endmembers.

BSE Composition Calculation

Element	Method
U abundance	McDonough & Sun (1995)-20.3ppb
Th & K abundances	Derived from Th/U and K/U ratios

5.1 Geoneutrino Flux: Three Earth Models

山东大学 SHANDONG UNIVERSITY

Reservoir	Geoneutrino flux at JNE (TNU)								
	Combined Model			ECM1			CRUST1.0		
	U	Th	$U+Th$	U	Th	$U+Th$	U	Th	$U+Th$
Sediment	$0.74^{+0.10}_{-0.10}$	$0.24^{+0.03}_{-0.03}$	$0.98^{+0.13}_{-0.13}$	$0.72^{+0.09}_{-0.09}$	$0.23^{+0.03}_{-0.03}$	$0.95^{+0.12}_{-0.12}$	$0.69^{+0.09}_{-0.09}$	$0.22^{+0.03}_{-0.03}$	$0.91^{+0.12}_{-0.12}$
Upper Crust	$28.39^{+7.24}_{-7.35}$	$7.38^{+1.18}_{-1.19}$	$35.77^{+8.36}_{-8.47}$	$24.06^{+6.18}_{-6.24}$	$6.22^{+0.99}_{-1.01}$	$30.29^{+7.06}_{-7.18}$	$28.34^{+7.21}_{-7.33}$	$7.35^{+1.17}_{-1.18}$	$35.69^{+8.33}_{-8.45}$
Middle Crust	$7.47^{+3.93}_{-3.85}$	$3.10^{+1.92}_{-1.86}$	$10.57^{+5.82}_{-5.70}$	$5.98^{+3.53}_{-3.49}$	$2.21^{+1.65}_{-1.61}$	$8.19^{+5.10}_{-5.06}$	$6.89^{+3.90}_{-3.74}$	$2.77^{+1.83}_{-1.79}$	$9.66^{+5.70}_{-5.51}$
Lower Crust	$1.11^{+0.68}_{-0.69}$	$0.72^{+0.52}_{-0.57}$	$1.83^{+1.20}_{-1.26}$	$1.66^{+1.11}_{-1.11}$	$1.04^{+0.82}_{-0.89}$	$2.70^{+1.95}_{-1.98}$	$0.97^{+0.61}_{-0.64}$	$0.57^{+0.40}_{-0.47}$	$1.54^{+1.02}_{-1.10}$
Crust (total)	$37.72^{+8.65}_{-8.67}$	$11.44^{+2.51}_{-2.51}$	$49.16^{+10.89}_{-10.85}$	$32.42^{+7.53}_{-7.53}$	$9.71^{+2.38}_{-2.34}$	$42.12^{+9.62}_{-9.54}$	$36.89^{+8.65}_{-8.48}$	$10.91^{+2.41}_{-2.39}$	$47.80^{+10.68}_{-10.65}$
Lithospheric Mantle	$1.67^{+1.31}_{-1.36}$	$0.55^{+0.45}_{-0.47}$	$2.23^{+1.75}_{-1.83}$	$1.03^{+0.69}_{-0.74}$	$0.34^{+0.24}_{-0.27}$	$1.37^{+0.93}_{-1.00}$	$1.68^{+1.32}_{-1.37}$	$0.56^{+0.45}_{-0.47}$	$2.24^{+1.75}_{-1.84}$
Lithosphere (total)	$39.40^{+9.20}_{-9.15}$	$11.99^{+2.72}_{-2.73}$	$51.39^{+11.57}_{-11.62}$	$33.44^{+7.70}_{-7.68}$	$10.05^{+2.40}_{-2.42}$	$43.49^{+9.76}_{-9.77}$	$38.58^{+9.11}_{-9.01}$	$11.46^{+2.66}_{-2.62}$	$50.04^{+11.41}_{-11.32}$
Depleted Mantle	$3.58^{+1.04}_{-1.02}$	$0.85^{+0.50}_{-0.48}$	$4.43^{+1.54}_{-1.50}$	$3.73^{+1.08}_{-1.07}$	$0.89^{+0.52}_{-0.50}$	$4.61^{+1.60}_{-1.57}$	$3.58^{+1.04}_{-1.02}$	$0.85^{+0.50}_{-0.48}$	$4.42^{+1.54}_{-1.50}$
Enriched Mantle	$4.23^{+1.84}_{-1.82}$	$0.95^{+0.61}_{-0.60}$	$5.18^{+2.43}_{-2.38}$	$4.28^{+1.86}_{-1.80}$	$0.97^{+0.61}_{-0.60}$	$5.24^{+2.41}_{-2.34}$	$4.23^{+1.84}_{-1.83}$	$0.95^{+0.61}_{-0.60}$	$5.18^{+2.43}_{-2.36}$
Total BSE	$\mathbf{47.20^{+8.68}_{-8.69}}$	$\mathbf{13.79^{+2.53}_{-2.54}}$	$\mathbf{60.99^{+10.91}_{-11.00}}$	$\mathbf{41.44^{+7.15}_{-7.23}}$	$\mathbf{11.90^{+2.22}_{-2.25}}$	$\mathbf{53.35^{+9.13}_{-9.25}}$	$\mathbf{46.38^{+8.52}_{-8.57}}$	$\mathbf{13.27^{+2.42}_{-2.44}}$	$\mathbf{59.64^{+10.64}_{-10.76}}$

5.2 The relationship between the geoneutrinoflux and radiogenic heat production.

Vary the total BSE uranium abundance between 6 and 40 ppb.

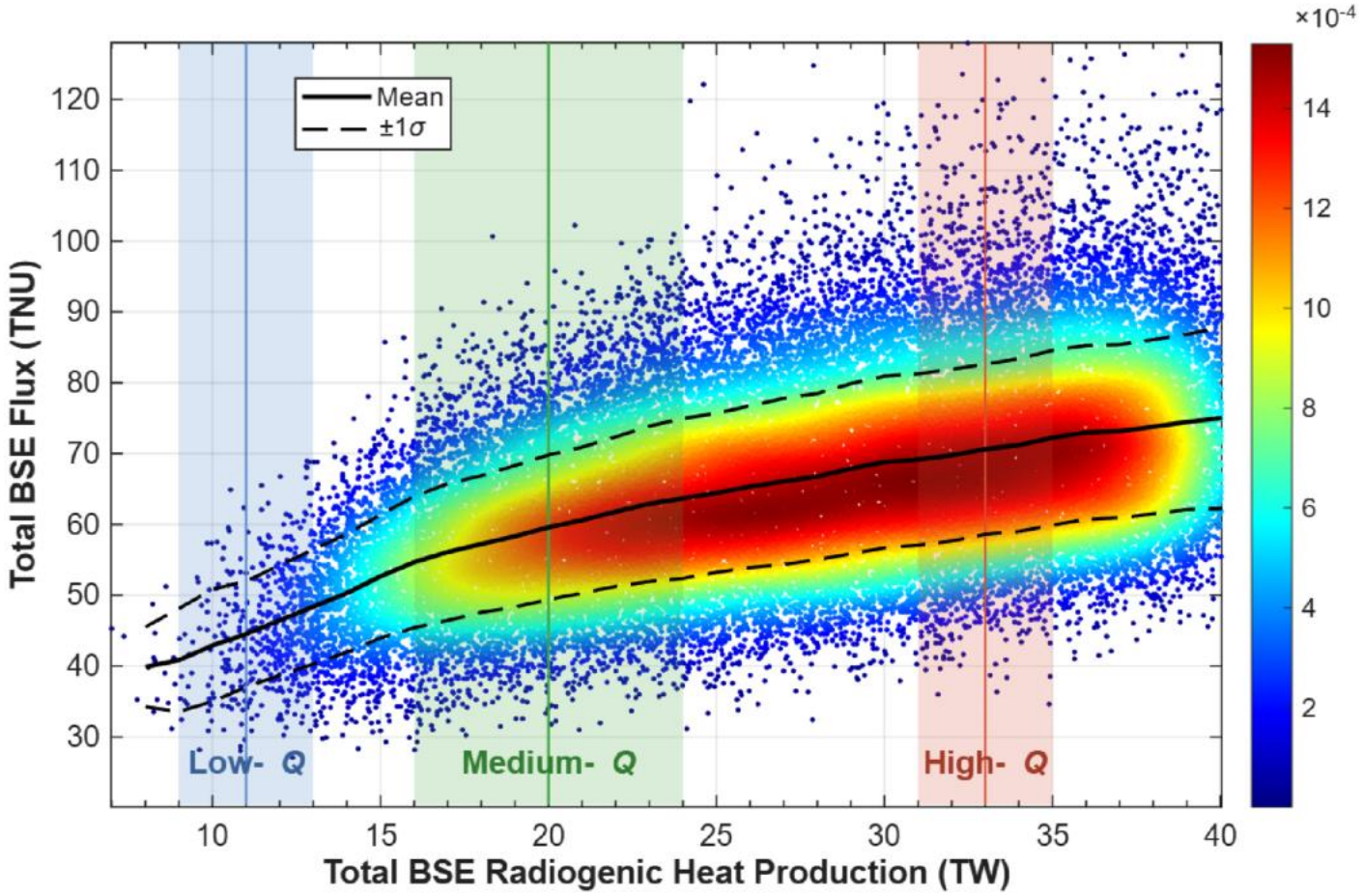

6.1 Reactor Background

Differential flux from a reactor:

$$\phi(E_{\bar{\nu}_e}) = \frac{W_{\text{th}} \cdot LF}{\sum_i f_i e_i} \sum_i f_i \, S_i(E_{\bar{\nu}_e})$$

Symbol	Meaning
W_{th}	Thermal power of reactor
LF	Load factor (= 1.0 in this study)
f_i	Fission fraction of isotope i ($\Sigma f_i = 1$)
e_i	Energy released per fission [MeV/fission]

Isotope	f_i	e_i [MeV/fission]
^{235}U	0.58	202.36 ± 0.26
^{238}U	0.07	205.99 ± 0.52
^{239}Pu	0.30	211.12 ± 0.34
^{241}Pu	0.05	214.26 ± 0.33

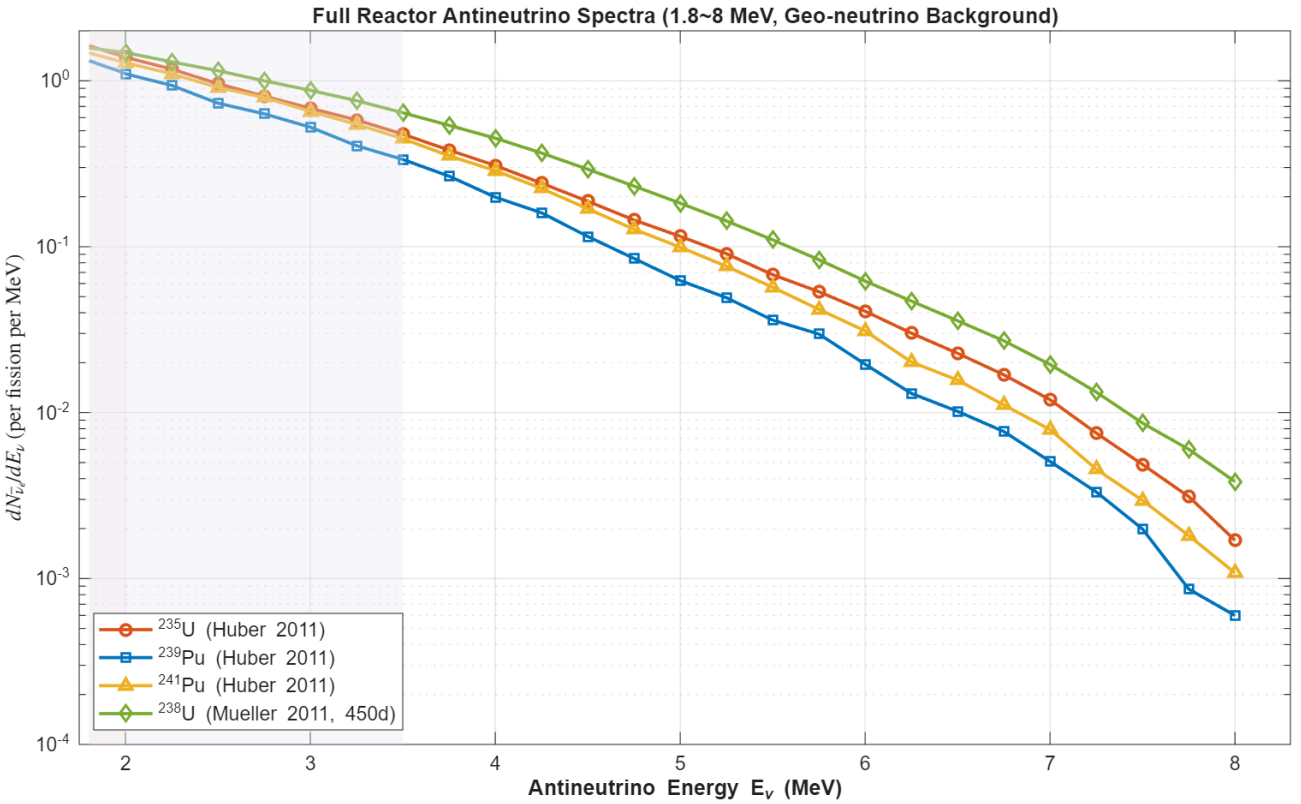

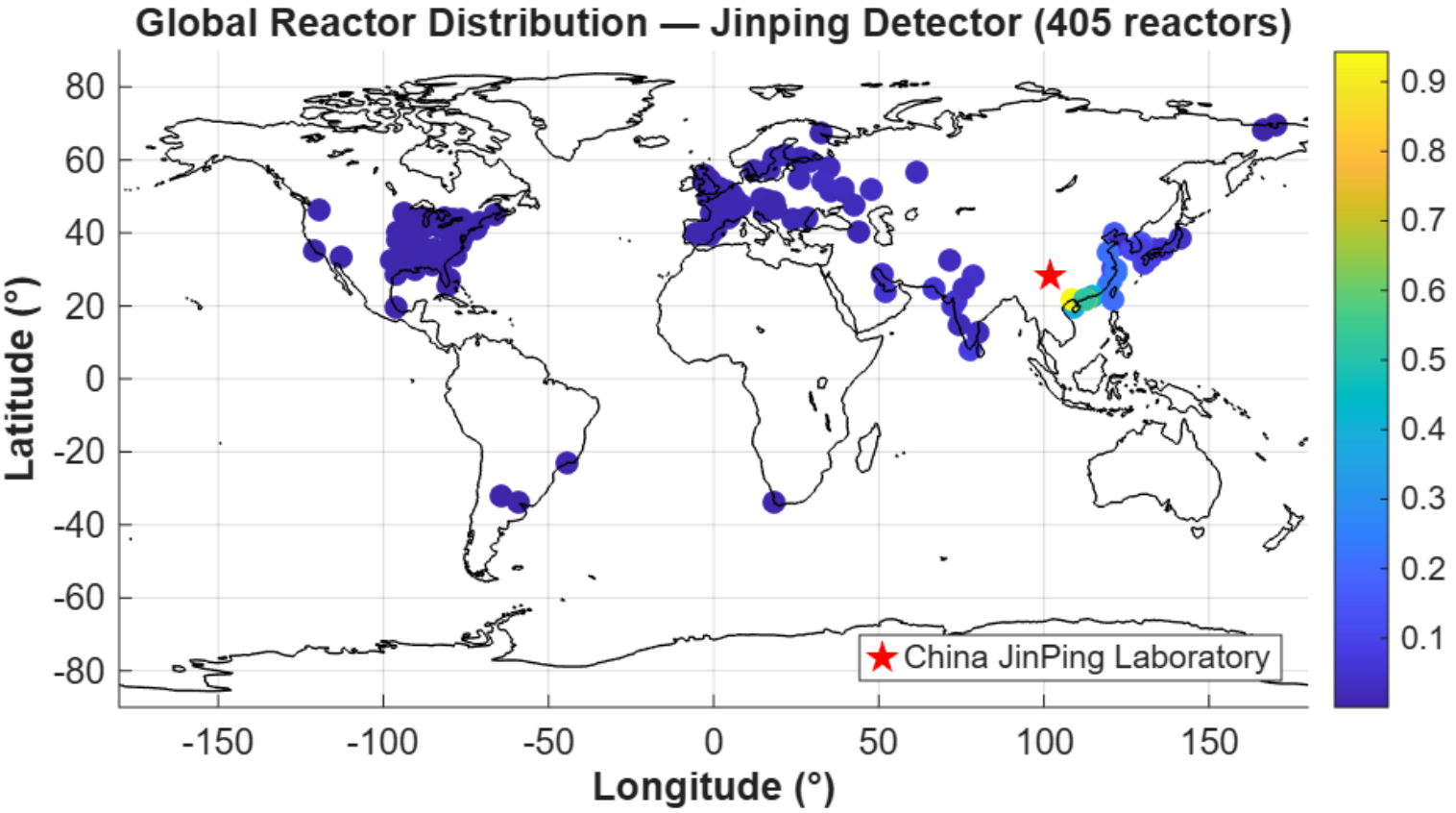
Global Reactor Distribution — Jinping Detector (405 reactors)
Latitude (°)
Longitude (°)
80
60
40
20
0
-20
-40
-60
-80
-150
-100
-50
0
50
100
150
0.9
0.8
0.7
0.6
0.5
0.4
0.3
0.2
0.1
China JinPing Laboratory

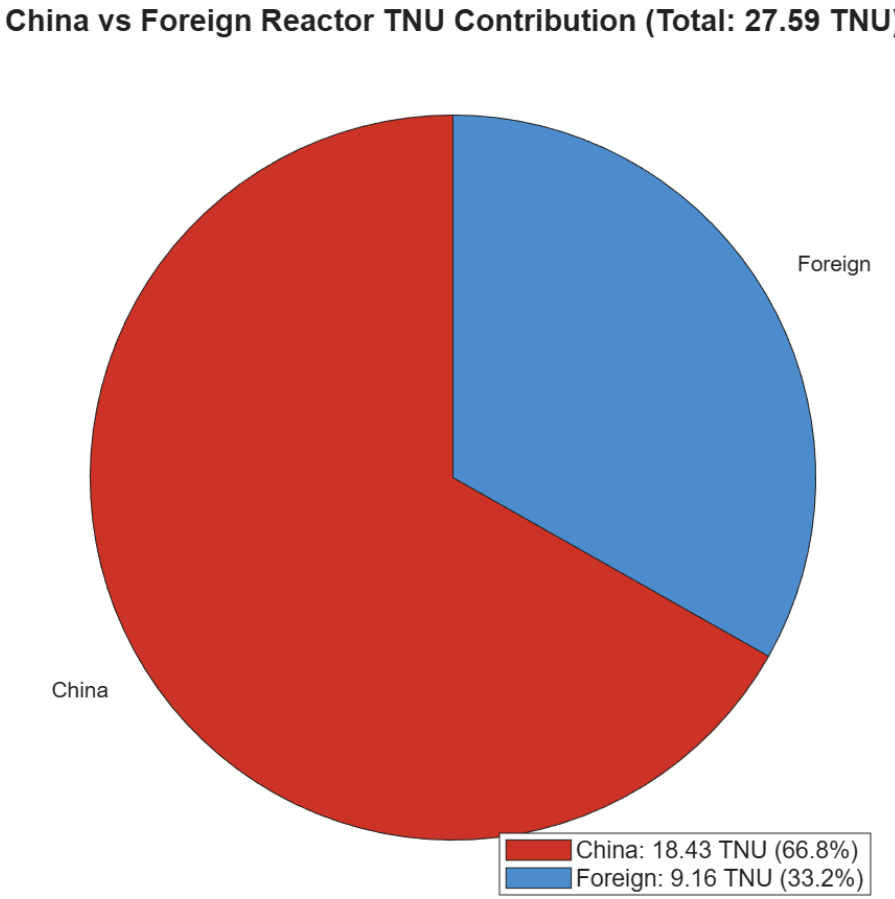
China vs Foreign Reactor TNU Contribution (Total: 27.59 TNU)
Foreign
China
China: 18.43 TNU (66.8%)
Foreign: 9.16 TNU (33.2%)

6.2 Total IBD Spectrum at JNE

FIG. 6. Predicted reactor antineutrino signal contributions, in TNU, at Jinping as a function of reactor–detector distance.

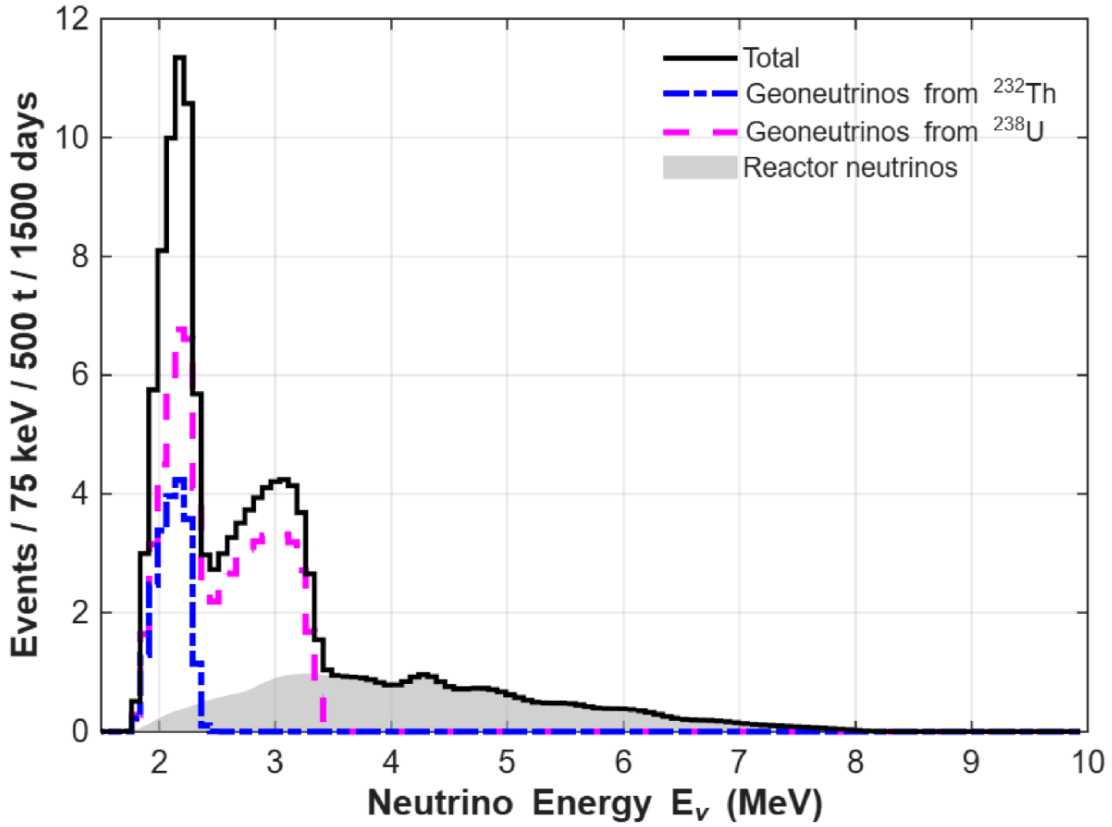

Event Rates (500 t × 1500 days)

	Geoneutrino			Reactor $\bar{\nu}_e$
	^{238}U	^{232}Th	^{238}U + ^{232}Th	
Event Rates (TNU)	47.20	13.79	60.99	27.59
Event Counts	69.78	20.39	90.18	40.78

7 Summary & Outlook

Jinping for Geoneutrino Detection

Advantage

Relatively low reactor background

→ Exceptionally favorable S/B ratio vs operating & proposed detectors

Challenge

Exceptionally complex crustal structure (Tibetan Plateau margin)

Thick crust → larger crustal signal uncertainty

Directions for Future Improvement

1. **U/Th abundances in the upper crust around CJPL** — primary contributor to total signal
2. More accurate estimation of U/Th in the middle and lower crusts (current Vp-based linear method is coarse)

山东大学
SHANDONG UNIVERSITY

Thank You